Title: Peri-somatic modulation of diffracted light and its variation with consciousness

Authors: Santosh A. Helekar[1, 2, *]

Affiliations: [1]Translational Biomagnetics and Neurometry Program and Department of Psychiatry and Behavioral Health, Houston Methodist Research Institute, Houston, Texas

[2]Department of Psychiatry, Weill Cornell Medicine, New York, New York

*Corresponding author. Email: sahelekar@houstonmethodist.org

Abstract

Existing noninvasive neurophysiological recording methods can acquire neuronal correlates of consciousness, but they do not differentiate between conscious and unconscious states mechanistically. Here we describe a method that detects a new physical effect of apparent neural origin in the peri-somatic space that might allow such differentiation. This effect is a slow decrease in the intensity of diffracted low power laser light emitted within a photoelectronic device placed close to the body of an awake subject. It is markedly attenuated by general anesthesia in mice and unconsciousness in patients. Its direction is reversed when the device is exposed to live invertebrates or to the decapitated head of a euthanized mouse. These findings reveal a previously unrecognized biophysical phenomenon that appears to be related to consciousness.

Main Text:

The existing methods of studying brain function rely on our understanding that neural information processing involves action potentials and synaptic transmission occurring within neuronal networks(*1*). These methods have greatly expanded neuroscientific knowledge of the underlying mechanisms of sensory processing, object representation, self and body image representation, processing of emotions, interoception and proprioception, memory storage and retrieval, volition and motor planning and action (*2-11*). However, they cannot yet clearly distinguish between conscious and unconscious brain activity or detect and measure the level of consciousness in any organism(*12-14*). The phenomenon of consciousness itself continues to elude a scientific explanation, despite having been the subject of intense philosophical and scientific debate for centuries(*12-14*)**.** Recently, a large-scale experimental effort to test two prominent theories of consciousness, Integrated Information Theory and Global Neuronal Workspace Theory, using functional magnetic resonance imaging, magnetoencephalography, and intraoperative electrophysiological recordings under an adversarial collaboration, yielded inconclusive results(*15*).

Neuroscientific investigations focus on the notions that neuronal electrical activity, computation in neural networks, mode of distribution of neural information, complexity of information processing, and/or predictive processing, are somehow responsible for conscious awareness or subjective experience(*16*). Nonetheless, the lack of progress in pursuing these avenues of research to obtain compelling evidence in support of these views has led to unconventional speculations, for example, involving a revival of old quantum theoretical ideas and new quantum proposals inspired by neurobiology(*17-19*). There is now growing evidence that quantum physicochemical processes play wide-ranging roles in biology, such as quantum superposition

and coherence in photosynthesis(*20*), inelastic electron tunneling in olfactory ligand-receptor interactions(*21*), and weak magnetic field effects on the radical pair mechanism in cryptochromes in avian migration(*22*). Other quantum effects include light harvesting and exciton diffusion in microtubules which is attenuated by general anesthetics(*23*), isotopic effects of xenon as an anesthetic(*24*) and increased fluorescence quantum yield in biological networks containing tryptophans(*25*). While these examples from the nascent field of quantum biology(*26*) offer a plausibility argument that quantum processes might play some role in the emergence of consciousness, this explanation has so far remained largely speculative in nature and devoid of clear testable psychophysical predictions.

Drawing inspiration from the repeated convergence of intuitions of prominent physicists, both historical and contemporary, on the connection between the mind and the measurement problem in quantum mechanics and the well-recognized central role of the light wave-particle duality at this interface, we tested whether proximity to human subjects and other animals might modulate in a readily detectable and reproducible manner light wave phenomena such as interference and diffraction and whether such modulation is affected by a change in the level of consciousness. We report here that, in recordings conducted with a simple photoelectronic device (described below and referred to as a Sentiometer) developed in our laboratory, placement of its sensor in the peri-somatic space for brief durations is associated with a marked distance-dependent change in the intensity of diffracted light, characterized by a decrease in human subjects and mice, and an increase in invertebrates. We also observe that the decrease is attenuated by general anesthesia in mice and unconsciousness due to brain injury in patients admitted to the intensive care unit (ICU). Furthermore, a decapitated mouse head shows a paradoxical increase in intensity. These observations suggest a possible relationship of the measured light wave intensity

modulation to the neural mechanism underlying consciousness and offer a potential new method to record and measure a correlate of the relative change in the conscious and unconscious activity of the brain.

A noninvasive photoelectronic instrument detects a new peri-cranial physical effect

We developed two versions of a new photoelectronic instrument, the Sentiometer, that measure either interference or diffraction of light waves emitted by a low power laser diode. Figure 1A shows a schematic diagram of the sensor module and its hypothetical principle of operation. The current working prototype used in the experiments described here is shown in Figure 1B. For each recording we powered the device by connecting it to a laptop computer (Fig. 1B) or an Android tablet and recorded the voltage output of four off-center photodiodes that sampled diffracted light in separate channels, using a serial monitor application that logged the data at the sampling rate of 100 Hz. All experiments began by recording the sentiometric baseline with no source of activity close to it within a radius of 180 cm for at least 30 min. It took 20 – 30 min for the baseline to stabilize at a constant level. Figure 1C shows a baseline recording of intensities from 4 off-center channels in an empty room after achieving a stable baseline, which shows no large amplitude deviations. A time series of scores of the first principal component of these data are shown in Figure 1D. In the first experiment, after 40 min we instructed each human subject to sit on a chair for 10 – 15 min such that his/her left temple was 1 cm from the sensor module. Sentiometric recordings from all channels during exposure of the head to the sensor module consistently showed a large decrease in intensity that peaked at the end of the exposure and declined gradually over ~30 min (Fig. 2A). Principal component analysis of the 4 off-center channel traces to measure the shared variance across all channels showed that >97% of their variance was accounted for by the first principal component. Therefore, we plotted a normalized

inverted version of this component as the final representation of the recorded effect in all subsequent experiments. We have expressed the strength of the recorded sentiometric response (SR) in arbitrary units (au). 10-min recordings from 7 healthy adult human subjects with the sensor module placed at 1 cm from the left temple revealed the strength of SR to be 601.4 ± 61.6 au (mean and standard error of the mean). To rule out any element of subjective bias in the recording of SR and in attributing it to actual exposure of the head to the device sensor, we conducted a double-blind experiment in which the subject who was alone in a closed room, sat at random on one of two chairs placed 90 cm apart (a distance at which little or no SR was detected). Each chair was fitted with either an active or an inactive device, indistinguishable to the subject. Using an electronic tablet the subject indicated the time and the chair on which he/she sat. The researcher conducting the experiment who was outside the closed room could find out whether the occurrence of the SR matched with the position of the subject only at the end of the experiment. In all recordings conducted in 5 subjects there was a perfect match between the SR and the position of the subject relative to the active device (Fig. 2B). We then tested the dependence of the SR amplitude on the distance between the sensor module and the head (left temple) by recording SRs at 9 different distances in two experiments, each conducted in 3 subjects. Figure 2C shows example recordings from one of these experiments and bar plots of mean amplitudes and standard errors of the mean (SEM) as a function of distance. The amplitude declines steeply with distance with a half maximal decrease of ~2.7 cm.

Spread of the physical effect is detected in the peri-somatic space

To investigate whether the measured physical effect can also be recorded close to the rest of the body, we exposed a hand to the sensor module of the Sentiometer at 1, 2, 4, 8 and 16 cm distance. We observed a peri-manual SR (n = 3) that was ~31% and significantly (p = 0.014,

two-tailed Student's paired t test, n = 3) reduced in amplitude to peri-cranial SR when the two were measured under the same conditions. It also declined with distance like the peri-cranial SR. Figure 2D shows traces and bar plots of peri-manual SR as in Figure 2C.

SR is not due to body heat, humidity, respired air, inaudible sound or electromagnetic fields

Experiments demonstrating that temperature changes due to body heat do not account for SR are described in Supplementary Materials. Descriptions of experiments ruling out any significant contributions from breathed air, displacement of air produced by inaudible sound or ultrasound waves, changes due to static magnetic field or radiofrequency electromagnetic waves are also provided in Supplementary Materials. All results of these experiments are shown in figs. S1 – S3.

SR is inverted in invertebrates compared to mammals

We asked whether other species of animals produce SR by exposing mice and 4 different invertebrates (blue crabs, California blackworms, crayfish and cherrystone clams) to the sensor module. Figure 3A shows that a mouse when exposed to the sensor module for 60 min at <5 cm evoked an SR like that in humans but of a smaller amplitude. A 60-min exposure in 10 mice produced a peak SR amplitude of 516 ± 32 au. The invertebrates, blue crabs (n = 9) and California blackworms (>200 in a clump) exposed for 60 min to the sentiometric sensor produced an inverted SR (Fig. 3A). Other invertebrates also produced an inverted response with a similar time course (fig. S4).

General anesthesia decreases the amplitude and shortens the rise time of SR in mice

Substantial evidence indicates that general anesthesia induces complete loss of consciousness(*28*). If the SR is produced by a mechanism that underlies, or is related to, consciousness, then all general anesthetics should significantly attenuate it. We tested this prediction with an inhalant anesthetic, isoflurane (If) and 3 injectable formulations – ketamine/xylazine (KX), pentobarbital (Pb), and propofol (Pf), administered intraperitoneally in mice. All anesthetics produced similar significant alterations in the time course and peak amplitude of the SR. The mean half-maximal rise time was ~44% shorter under anesthesia (7.6 ± 0.4 min, n = 4 for KX; 11.3 ± 0.6 min, n = 4 for If) than in the pre-anesthesia waking state (14.9 ± 1.0 min for KX; Fig. 3B; 19.9 ± 1.2 min, n = 4 for If; Fig. 3C). The mean amplitudes at 60 min were ~42% lower under anesthesia (353 ± 61 au, n = 4 for KX; Fig. 3B; 266 ± 16 au, n = 4 for If; Fig. 3C) than before anesthesia (535 ± 39 au, n = 4 for KX; Fig. 3B; 490 ± 19, n = 4 for If; Fig. 3B). These differences were statistically significant for both the rise time (p = 0.005, n = 4 for KX; p = 0.012, Student's paired t test, n = 4 for If) and amplitude (p = 0.014, n = 4 for KX; p = 0.0018, Student's paired t test, n = 4 for If). These effects reversed with recovery except for the decrease in amplitude with KX over the duration of the experiment, likely due to its prolonged blocking action on NMDA receptors(*29*). The decreases in amplitude at 60 min and rise time showed small differences in values between the four types of anesthetics (see fig. S4B for Pb and Pf effects). We also carried out continuous sentiometric recordings in mice (n = 3) before (~55 min), during (~55 min) and after (~70 min) administration of If general anesthesia to monitor the transition from the awake state to the anesthetized state and the recovery from the latter state to normal wakefulness over a period of 3 hours. Each mouse was kept in a loose restraining tube inside the anesthesia chamber supplied with O_2 and CO_2 or air throughout the recording. The flow of If into the chamber was started at ~55 min after the start of exposure of the awake mouse to the sensor and stopped ~55 min later. Figure 3D shows a representative recording from this

experiment. The recorded baseline amplitude declines during anesthesia compared to the pre-anesthesia awake state and takes >60 min to start rising again to return to the pre-anesthesia level during recovery.

Bidirectional SR in the decapitated head of euthanized mice

In a rodent, neuronal electrical activity ceases <30 s after the last electrocardiographic signal, as indicated by electroencephalographic (EEG) recordings*(30)*. In dying human patients EEG has been reported to become isoelectric as early as a few minutes before the last heartbeat*(31)*. However, it is unlikely that any neuron within the brain would still be electrically active hours after complete cessation of cerebral blood flow and perfusion. If neuronal electrical excitation is required for the underlying process that produces an SR then sentiometric recording conducted after euthanasia in mice should show the complete disappearance of the SR at a certain latency after the cessation of the heartbeat. The duration of the latency will likely be in the range of 60 – 90 min, given the slowness (see above) of the time course of the effect that originated before death. We performed euthanasia by carbon dioxide inhalation and recorded the SR to 60-min exposures of mice to the sentiometric sensor before and after euthanasia. As predicted, a 60-min exposure beginning at 5 min after cessation of the heartbeat showed a decaying SR (Fig. 4). The mean peak amplitude of this SR was (280 ± 13, n = 3) au, 54 % of the mean amplitude of the SR before euthanasia induction (531 ± 65 au, n = 3). A 60-min recording from 110 min to 170 showed little or no measurable SR. As in the case of general anesthesia, the half maximal rise time showed a 49% reduction in the postmortem SR (8.1 ± 0.3 min, n = 3) compared to the SR before death (17.2 ± 2.9 min, n = 3). However, when we decapitated the mouse after euthanasia and exposed it and the head and body separately but at the same time to sensor modules of two different Sentiometers, we observed a peri-cranial SR that was initially biphasic (between 5 and

65 min) and then inverted (between 110 and 170, n = 5, Fig. 4D). In contrast to the head, the headless body showed a decaying response at the 5-min onset time after clinical death, with the sentiometric recording becoming nearly isoelectric at the 110-min postmortem time point. Persistence of the peri-cranial SR at >110 min when there is little or no SR produced by the headless body strongly suggests that the SR primarily, if not exclusively, originates in the brain in mice and passively spreads to the rest of the body where it may be amplified because of its larger volume compared to the head. This prolonged persistence after death also suggests that the source of the peri-cranial SR is unlikely to be neuronal electrical activity.

Unresponsive patients with primary brain injury show reduced SR and restoration with recovery

To examine whether the amplitude of SR is reduced in unresponsive and clinically presumed unconscious adult patients with primary brain injury due to any cause, we conducted 2 – 3 recordings of 30-min peri-manual SR on different days in each of 3 patients being treated in the ICU. The first patient (a 69-year-old male) had acute encephalopathy supervening on Parkinson's disease with dementia (PDD). He recovered from the acute condition over several days. The second patient (a 47-year-old male) suffered from severe intracerebral hemorrhage and remained in the same state as determined clinically over the period during which the recordings were conducted. The third patient (a 75-year-old male) had a large subdural hematoma and remained clinically unresponsive and unconscious during our recordings. None of the patients received sedatives. Their results were compared with those obtained from 1 – 3 recordings carried out in 4 conscious healthy adults (2 males and 2 females) under the same conditions in the ICU. As shown in Figure 5A, the first recordings in all three patients (251 ± 110 au) showed significant reduction in mean peak SR amplitude compared to the mean peak SR amplitude in

the healthy controls (667 ± 84 au, n = 4, p = 0.027, Student's pooled t test). Subsequent recordings in each patient are shown in Fig. 5B. The first patient showed a progressive increase in peak SR amplitude with clinical recovery, achieving a normal-appearing SR 9 days after the initial nearly flat SR. The other two patients showed slight progressive reduction of the peak amplitude, consistent with lack of change in their clinical condition. As seen in the prior recordings in human subjects and mice, in the awake state, SR does not decline until its source (e.g., hand, head or body) is removed from the proximity of the sentiometric sensor. By contrast, a noteworthy common feature in all three patients is the premature decline of the SR with or without the occurrence of more than one peak before the removal of the hand. This observation suggests an inability of the injured brain of these patients to maintain a high constant level of consciousness, assuming that the SR amplitude reflects this level. Sentiometric data from these patients and healthy controls also allowed us to again test whether the SR is simply caused by the change in temperature due to body heat. The SR peak amplitudes ranged from 31.5 au through 758.3 au. However, the corresponding body temperatures measured clinically in patients varied in the normal range only from 97.6^{o}F through 98.7^{o}F. We correlated the patients' body temperatures with the highest peak amplitude of their SRs on each day of recording and found that there was no significant correlation between them (r = -0.1, p = 0.74, Pearson's correlation analysis, Fig. 5C), confirming that changes in body temperature cannot account for the changes in SR amplitude.

Discussion

Our experiments demonstrated: first, that light emitted by a low power laser LED when placed near the body of a living organism is correlated with a striking, easily measured, and reproducible change in the intensity of the amount of light that is diffracted. The change takes

>20 min to rise to a maximum and, upon moving the device away from its source, to decline to the baseline. It is bidirectional, with the direction of change being dependent on the type of organism that is exposed to the device sensor, i.e., the intensity decreases in human subjects and mice and increases in several invertebrates. Second, the amplitude of the SR, representing the amount of change in intensity declines with distance from the body. Third, two kinds of variations in the level consciousness are associated with qualitative and quantitative changes in SR. General anesthesia in mice is correlated with a faster rise and reduced amplitude of the SR, with recovery resulting in restoration of the rise time, and in some cases also the amplitude, to that seen in the awake state. Furthermore, exposure of a decapitated head from a euthanized mouse to the sensor module of a Sentiometer results in a biphasic SR initially and then an inverted SR that persists for ~3 hours after death. In ICU patients who are clinically unresponsive and unconscious due to a primary brain injury or impairment, the SR is substantially attenuated and shows a premature decline, despite persistent exposure. In one patient, a virtually absent SR dramatically returned to normal when the patient recovered clinically. These findings provide evidence for a previously unrecognized biophysical effect detectable in the peri-somatic space, which appears to originate in the brain. The effect's amplitude is modulated by changes in the level of consciousness, with its direction of modulation being determined by the viability of the mammalian brain and its source being invertebrates as opposed to mammals.

The underlying cause of this newly discovered phenomenon is not clear at present. We have been able to rule out contributions from known factors such as electromagnetic emissions, humidity, breathed air, sound and ultrasound, and heat transfer by conduction and convection from the body. Body heat transfer by radiation cannot also account for the SR because of the results of the

experiments with the water bath and the lack of correlation of the large variations in SR amplitude in patients and healthy controls with their body temperature that varied slightly within the normal range. However, given that temperature does have some influence on sentiometric recordings, it is possible that a presently unknown classical mechanism analogous to radiative heat transfer is responsible for modulating the intensity of diffracted light waves.

An alternative possibility is that the effect involves a quantum process, for example like that involving the spontaneous collapse of wavefunctions in neuronal microtubules proposed by Penrose and Hameroff(*32*), which somehow spreads in space causing the collapse or decoherence of laser light waves. A third alternative might be a quantum process at the source within neurons spreading spatially through a non-quantum classical process. Which of these hypotheses or some other entirely different explanation might account for the sentiometric effect awaits further investigation. But we can at least conclude here that sentiometry with the noninvasive photoelectronic device developed in our laboratory could serve as a new neurophysiological technique to probe the level of consciousness in both basic and clinical neuroscience.

Materials and Methods

Description of the Sentiometer

We designed and constructed 2 versions of a photoelectronic Sentiometer involving a sensor module containing a low power 5 mW, 650 nm, 3 mm aperture red dot laser light-emitting diode (LED) without an automatic power control circuit, and up to 5 photodiodes. The sensor module in each version is connected to a microcontroller board (STM32, DIANN, China) with a 12-bit analog to digital converter. Version 1 sensor module has a partition containing a vertical double

slit (1 mm width slits separated by 2 mm) placed between the laser LED and a horizontal array of 5 photodiodes, which produces an interference pattern. The photodiodes sample the bright interference bands. In version 2, 4 photodiodes form the vertices of a quadrilateral around a central photodiode. The outer photodiodes sample the diffracted light waves emerging from the laser LED.

Data acquisition and display

The analog channel output from all photodiodes was fed into the analog pins of STM32 and digitized at 12 bits on a 0 – 4095 scale. The digital output sampled at 100 Hz was streamed and logged with a serial monitor program (Serial USB Terminal version 1.55 on Android tablet, Kai Morich; CoolTerm version 2.0.1, Roger Meier on Windows 11 PC). The raw voltage values from the 4 outer channels representing diffracted beams were subjected to principal component analysis to obtain the component of their baseline deviations that is shared across all channels by the highest amount (1st principal component score), which amounted to >97% in all recordings. A further normalization step of this first principal component score time series involved subtraction of its amplitude at each time point from its first time point, which resulted in an inversion of all values. The inversion allowed us to depict the amount of intensity decrease as a positive response whose amplitude represented its strength. The displayed plot of amplitude as a function of time was a smoothed running average of the amplitudes over 1 – 5 s in all figures. All data transformations and plotting were done using scripts written in house using the MATLAB (Mathworks, Inc., Natick, MA, USA) technical computing language.

Exposure of sentiometric sources to the sensor module of the Sentiometer

Procedures involving healthy human volunteers and unresponsive patients were performed under protocols approved by Houston Methodist Research Institute (HMRI) institutional review board (IRB). Informed consent forms signed by the volunteers and the authorized legal representatives of the patients were also approved by the IRB. Experiments involving mice (BALB/c mice obtained from The Jackson Laboratory, Bar Harbor, ME, USA) were approved by the HMRI institutional animal care and use committee. In all experiments a 30 – 45 min baseline was recorded before and after each exposure of a sentiometric source. In human subjects, exposure of the head to the sensor module at 1 – 30 cm involved the left or right temple just above the ear. Exposure of the left or right hand involved the palmar surface at similar distances. In the ICU recordings the hand was positioned at 15 cm from the sensor module on a plastic frame during the pre-exposure and post-exposure 45-min baseline recordings. The actual response to exposure of the hand was recorded by placing the hand at 1 cm above the sensor module on the plastic frame. Exposure of mice, or their decapitated heads, was carried out by lightly restraining each live mouse, or placing a dead mouse or head, in a perforated plastic tube with a 4-cm diameter to allow limited front and back, side to side and up and down movement of the mouse and free movement of air. The tube was placed directly over the sensor module, or in the case of the isoflurane (2%) anesthesia experiments, inside the anesthesia chamber placed above it. For injectable anesthetics, the intraperitoneal route was used (sodium pentobarbital 70 mg/kg, propofol 100 mg/kg and ketamine 100 mg/kg xylazine 18 mg/kg). The distance of the mouse from the sensor module was less than 5 cm. Crabs, crayfish and clams were placed one at a time in a closed polypropylene container. The container was then placed over the sensor module. Before exposure of the animal in the container to the sensor module we exposed the empty closed container itself to the sensor module to make sure that it did not induce an SR. Exposure of California blackworms was done by pouring a clump (containing >200 worms) of them along

with the water in which they were shipped by the vendor (Carolina Biological Supply Company, Burlington, NC, USA) into a polyethylene bag and holding the bag over the sensor module at 1 cm. The bag with the water alone was exposed to the module as control to make sure it was ineffective in inducing an SR. All recordings were done at room temperature, except in experiments done to measure the effect of temperature.

Data Analysis

Measured quantitative SR parameters were mean peak amplitude and half-maximal rise time. Statistical comparison of these parameters between different conditions was done using two-tailed Student's t tests. In the ICU recordings Pearson's correlation analysis was done on the SR and body temperature values.

References and Notes

1. C. Seguin, O. Sporns, A. Zalesky, Brain network communication: concepts, models and applications. *Nat Rev Neurosci* **24**, 557-574 (2023).
2. A. Azarfar, N. Calcini, C. Huang, F. Zeldenrust, T. Celikel, Neural coding: A single neuron's perspective. *Neurosci Biobehav Rev* **94**, 238-247 (2018).
3. N. E. Barraclough, D. I. Perrett, From single cells to social perception. *Philos Trans R Soc Lond B Biol Sci* **366**, 1739-1752 (2011).
4. C. Libedinsky, Comparing representations and computations in single neurons versus neural networks. *Trends Cogn Sci* **27**, 517-527 (2023).
5. F. Castro *et al.*, From rubber hands to neuroprosthetics: Neural correlates of embodiment. *Neurosci Biobehav Rev* **153**, 105351 (2023).

6. Z. Dary *et al.*, Neural bases of the bodily self as revealed by electrical brain stimulation: A systematic review. *Hum Brain Mapp* **44**, 2936-2959 (2023).

7. T. Engelen, R. Mennella, Piecing together the puzzle of emotional consciousness. *Neurosci Conscious* **2023**, niad005 (2023).

8. T. Engelen, M. Solca, C. Tallon-Baudry, Interoceptive rhythms in the brain. *Nat Neurosci* **26**, 1670-1684 (2023).

9. P. D. Marasco, J. C. de Nooij, Proprioception: A New Era Set in Motion by Emerging Genetic and Bionic Strategies? *Annu Rev Physiol* **85**, 1-24 (2023).

10. S. Tonegawa, M. Pignatelli, D. S. Roy, T. J. Ryan, Memory engram storage and retrieval. *Curr Opin Neurobiol* **35**, 101-109 (2015).

11. E. Bizzi, R. Ajemian, From motor planning to execution: a sensorimotor loop perspective. *J Neurophysiol* **124**, 1815-1823 (2020).

12. L. Melloni, L. Mudrik, M. Pitts, C. Koch, Making the hard problem of consciousness easier. *Science* **372**, 911-912 (2021).

13. D. J. Chalmers, The problems of consciousness. *Adv Neurol* **77**, 7-16; discussion 16-18 (1998).

14. S. Paulson, D. Chalmers, D. Kahneman, L. Santos, N. Schiff, The thinking ape: the enigma of human consciousness. *Ann N Y Acad Sci* **1303**, 4-23; discussion 24 (2013).

15. M. Lenharo, Decades-long bet on consciousness ends - and it's philosopher 1, neuroscientist 0. *Nature* **619**, 14-15 (2023).

16. A. K. Seth, T. Bayne, Theories of consciousness. *Nat Rev Neurosci* **23**, 439-452 (2022).

17. A. J. Leggett, The quantum measurement problem. *Science* **307**, 871-872 (2005).

18. J. M. Schwartz, H. P. Stapp, M. Beauregard, Quantum physics in neuroscience and psychology: a neurophysical model of mind-brain interaction. *Philos Trans R Soc Lond B Biol Sci* **360**, 1309-1327 (2005).

19. R. Penrose, Uncertainty in quantum mechanics: faith or fantasy? *Philos Trans A Math Phys Eng Sci* **369**, 4864-4890 (2011).

20. A. Chenu, G. D. Scholes, Coherence in energy transfer and photosynthesis. *Annu Rev Phys Chem* **66**, 69-96 (2015).

21. M. I. Franco, L. Turin, A. Mershin, E. M. Skoulakis, Molecular vibration-sensing component in Drosophila melanogaster olfaction. *Proc Natl Acad Sci U S A* **108**, 3797-3802 (2011).

22. P. J. Hore, H. Mouritsen, The Radical-Pair Mechanism of Magnetoreception. *Annu Rev Biophys* **45**, 299-344 (2016).

23. A. P. Kalra *et al.*, Electronic Energy Migration in Microtubules. *ACS Cent Sci* **9**, 352-361 (2023).

24. N. Li *et al.*, Nuclear Spin Attenuates the Anesthetic Potency of Xenon Isotopes in Mice: Implications for the Mechanisms of Anesthesia and Consciousness. *Anesthesiology* **129**, 271-277 (2018).

25. N. S. Babcock *et al.*, Ultraviolet Superradiance from Mega-Networks of Tryptophan in Biological Architectures. *J Phys Chem B* **128**, 4035-4046 (2024).

26. H. Neven *et al.*, Testing the Conjecture That Quantum Processes Create Conscious Experience. *Entropy (Basel)* **26**, (2024).

27. F. Zapata *et al.*, Human ultra-weak photon emission as non-invasive spectroscopic tool for diagnosis of internal states - A review. *J Photochem Photobiol B* **216**, 112141 (2021).

28. M. B. Kelz, G. A. Mashour, The Biology of General Anesthesia from Paramecium to Primate. *Curr Biol* **29**, R1199-R1210 (2019).

29. S. Ma *et al.*, Sustained antidepressant effect of ketamine through NMDAR trapping in the LHb. *Nature* **622**, 802-809 (2023).

30. J. Borjigin *et al.*, Surge of neurophysiological coherence and connectivity in the dying brain. *Proc Natl Acad Sci U S A* **110**, 14432-14437 (2013).

31. G. Xu *et al.*, Surge of neurophysiological coupling and connectivity of gamma oscillations in the dying human brain. *Proc Natl Acad Sci U S A* **120**, e2216268120 (2023).

32. S. Hameroff, R. Penrose, Consciousness in the universe: a review of the 'Orch OR' theory. *Phys Life Rev* **11**, 39-78 (2014).

33. F. Zapata et al., Human ultra-weak photon emission as non-invasive spectroscopic tool for diagnosis of internal states - A review. J Photochem Photobiol B 216, 112141 (2021).

Acknowledgments: The author thanks Blessy John and Alvin Saldon for constructing the Sentiometers, Blessy John, Lisa Nguyen, Shashank Hambarde and Arvind Pandey for assisting with the human and animal experiments, Anh Nguyen for providing access to ICU patients, and Jayant S. Vaidya and Ronald Fisher for extensive discussions on the study experiments and results. This work was supported in part by anonymous philanthropic research funding provided to the author to conduct scientific research on consciousness.

Funding: This work was supported in part by anonymous philanthropic research funding provided to the author to conduct scientific research on consciousness.

Author contributions:

Conceptualization: SAH

Methodology: SAH

Investigation: SAH

Visualization: SAH

Funding acquisition: SAH

Project administration: SAH

Supervision: SAH

Writing – original draft: SAH

Writing – review & editing: SAH

Competing interests: SAH is listed as the inventor of the Sentiometer on patent applications filed by Houston Methodist Hospital.

Data and materials availability: All analyzed data are available in the main text or the supplementary materials. The MATLAB code and raw data logged from the recordings are available upon request.

Supplementary Materials

Supplementary Text

Figs. S1 to S4

References

Figure Captions

Fig. 1. Sentiometer Prototype Description and Operation

A. A schematic diagram showing the operation of the version 2 Sentiometer. **B.** An image showing the components of the Sentiometer: 1 – sensor module/unit, 2 – controller and 3 – Laptop computer. **C.** Raw sensor output channel recordings in an empty room. **D.** Normalized first principal component score time series derived from **C**.

Fig. 2. Peri-somatic Sentiometric Response (SR)

A. The Sentiometer sensor unit when brought close to the head (yellow boxes represent the timing and duration of exposure) in an awake subject produces a robust deviation of the time series away from the baseline with a slow time course of ~40 min [Left – raw channel recordings, **Right** – normalized first principal component score time series representing the sentiometric response (SR)]. Note that the normalization step renders a decrease in diffracted light intensity to be represented as an increase in amplitude of the SR. This convention is used in all figures below. **B.** A double-blind experiment with active and inactive devices shows the expected result. **C.** and **D.** SRs are shown varying as a function of distance. The bar plot data is derived from n = 3 each for peri-cranial and peri-manual SRs. The error bars depict standard

errors of the mean (SEM) in this and all figures below. Images in the figure are obtained from the stock image database of licensed BioRender software.

Fig. 3. Differences in SR Produced by Other Living Organisms and General Anesthesia

A. Peri-somatic SR recordings at ~1 cm with another mammal, mouse (n = 20) and invertebrates, blue crab (n = 9) and California blackworm (a clump of >200). Mice show upright SRs comparable to humans. Invertebrates show inverted SRs. **B.** Peri-somatic SRs (at <3 cm) before, during and after general anesthesia in mice loosely restrained in a plastic tube for a 60-min exposure. Ketamine and xylazine combination was administered intraperitoneally at 100 mg/kg and 18 mg/kg, respectively (n = 4). **C.** Isoflurane gas was administered at 2% in a small animal anesthesia chamber (n = 3). The bar plots depict means and SEMs of 60-min amplitude and half maximal rise times corresponding to the 3 conditions. Recovery from anesthesia is better seen in half maximal rise time, and not in amplitude. **D.** Continuous recording of the SR from a mouse exposed to the sensor at ~5 cm before (~55 min, pink box), during (~55 min, green box) and after Isoflurane (~70 min, orange box) general anesthesia. The arrows mark the start and end times of exposure and the on and off times of isoflurane flow into the anesthesia chamber. Images in the figure are obtained from the stock image database of licensed BioRender software.

Fig. 4. Decline of Peri-somatic SR and Inversion of Peri-cranial SR After Death

A. Peri-somatic and peri-cranial SRs in mice before and after euthanasia. The sentiometric sensor unit was exposed to the whole body of each mouse at <3 cm in a tube restrainer for 60 min (n = 5). Euthanasia was performed in a carbon dioxide chamber. **B.** The bar plot depicts means and SEMs of 60-min amplitudes before and immediately (5 – 65 min) after death. **C.** and **D.** SRs of the decapitated body (n = 3) and head (n = 3), respectively, at the same two

postmortem time points using two different Sentiometers. Images in the figure are obtained from the stock image database of licensed BioRender software.

Fig. 5. Unconsciousness due to Primary Brain Injury is Associated with Alteration of SR Amplitude and Time Course

A. Peri-manual SRs to 30-min exposure to the sensor unit in awake conscious healthy adults (n = 4) and unconscious adult patients with injury to the brain (n = 3) admitted to the intensive care unit (ICU). The bar plot, representing means and SEMs, shows statistically significant ~72% reduction in the peak amplitude of the SR in patients compared to conscious healthy adults. **B.** Peri-manual SRs obtained on different days during each of the three patients' stay in the ICU. The short red arrows point to the premature decline of the SR in all three patients before the termination of the peri-manual exposure. The dates of the recordings are indicated in the graph labels. The recording in gray is from the conscious healthy adult 3 from **A**. **C.** A graph of recorded peak SR amplitudes versus body temperatures in all patients and two healthy adults in whom temperature readings were available, showing no correlation between the two variables.

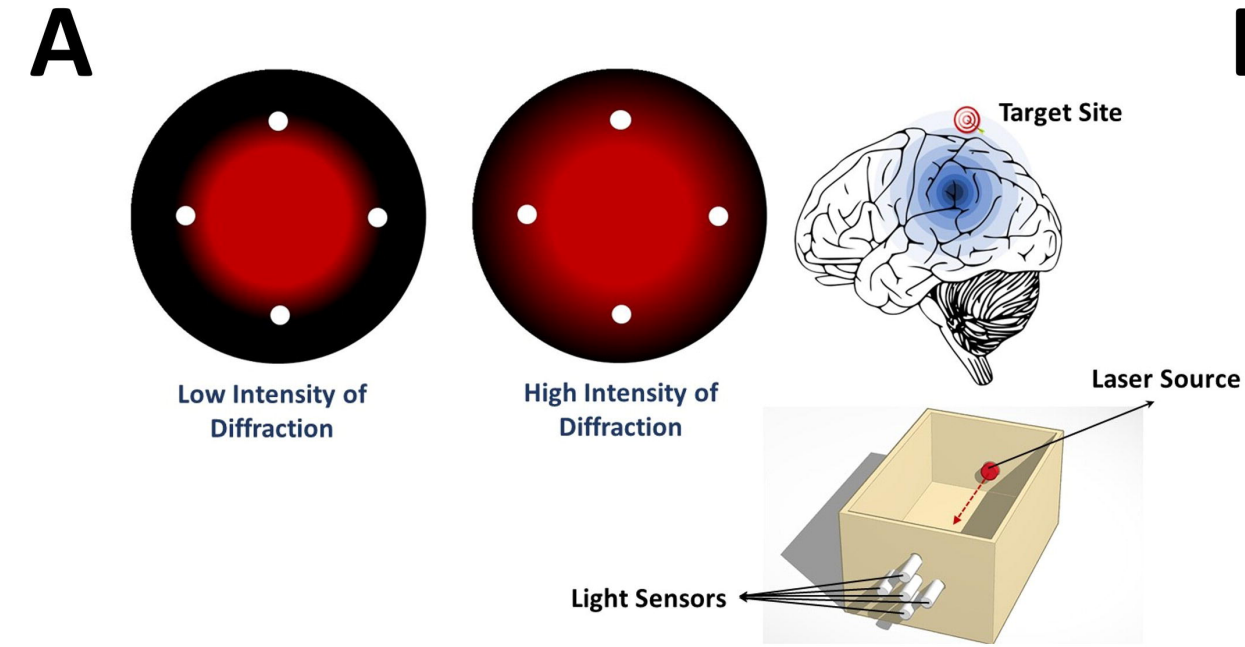
A
Low Intensity of Diffraction
High Intensity of Diffraction
Target Site
Laser Source
Light Sensors

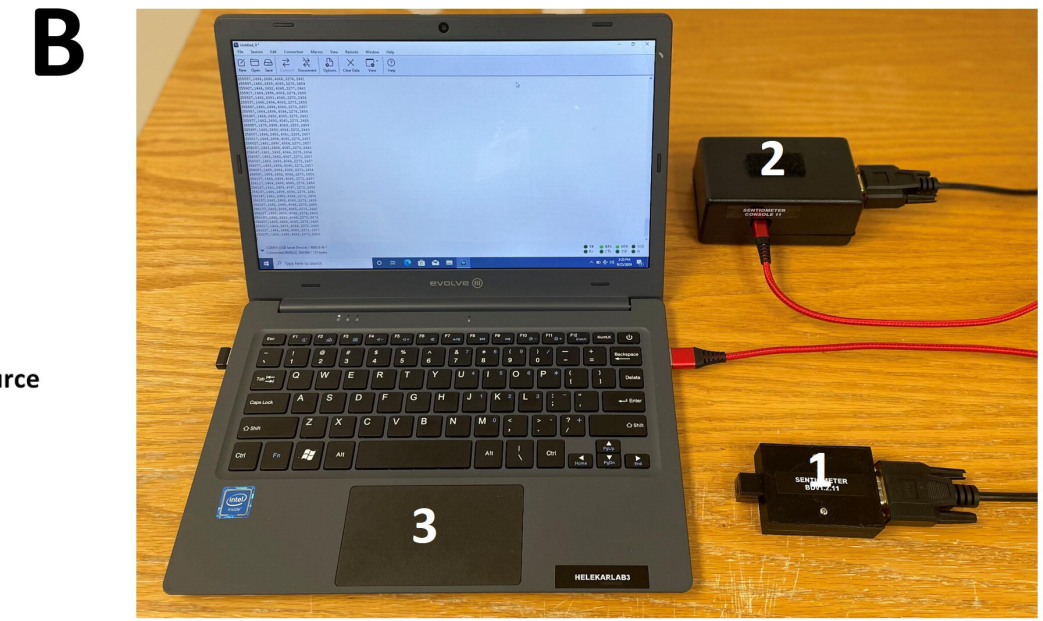
B
2
1
3
HELEKARLAB3

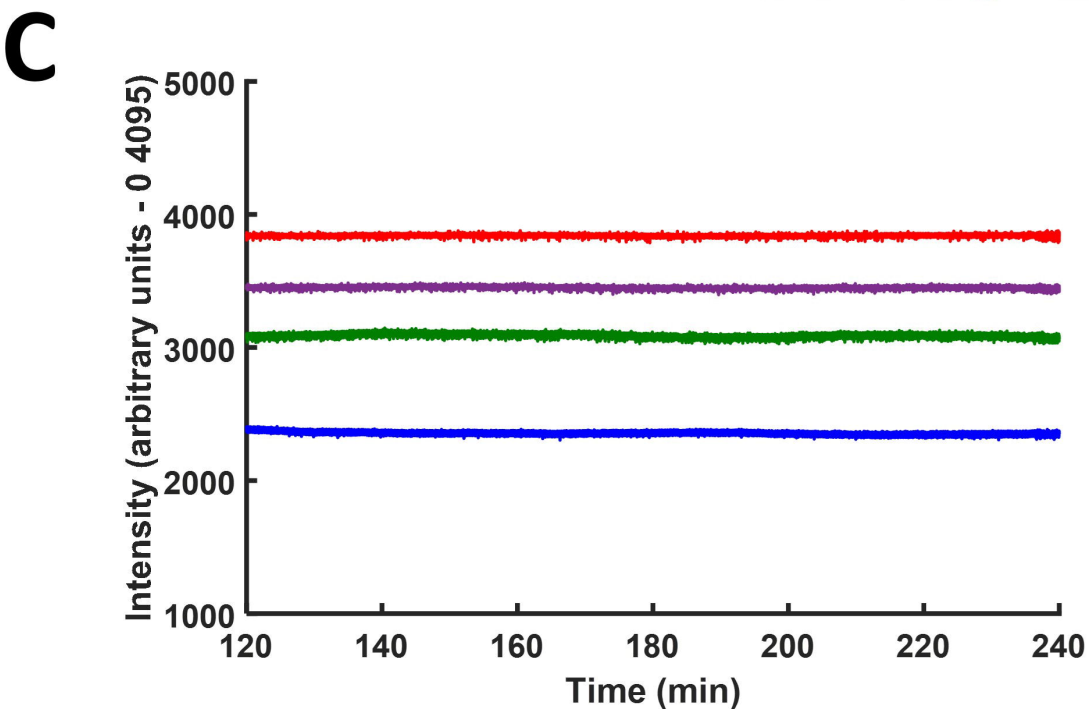
C
Intensity (arbitrary units - 0 4095)
5000
4000
3000
2000
1000
120
140
160
180
200
220
240
Time (min)

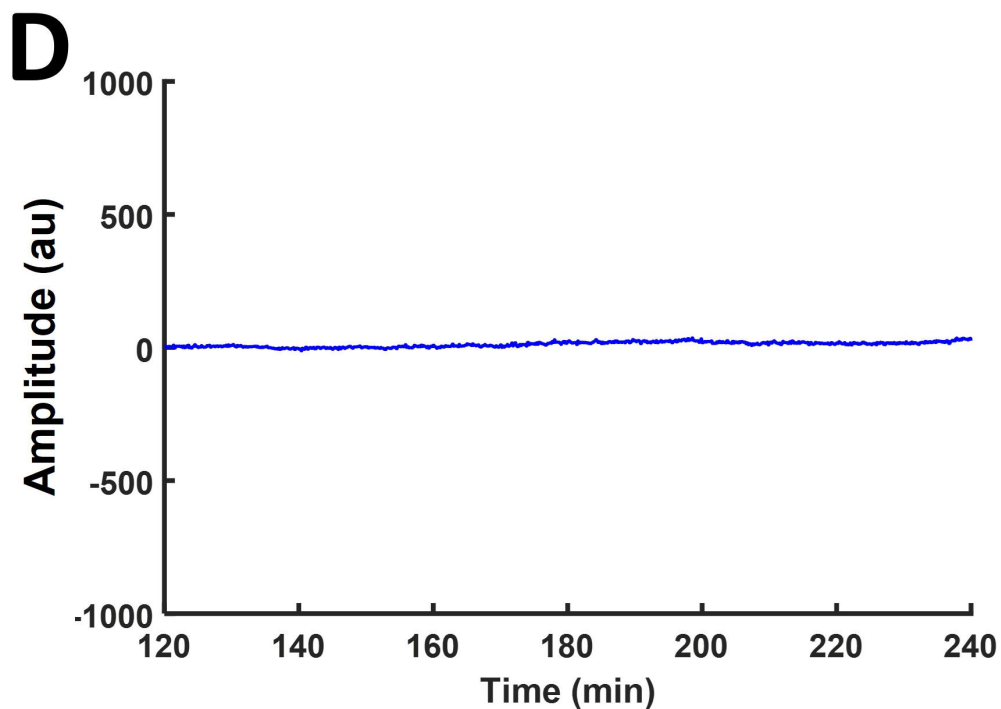
D
Amplitude (au)
1000
500
0
-500
-1000
120
140
160
180
200
220
240
Time (min)

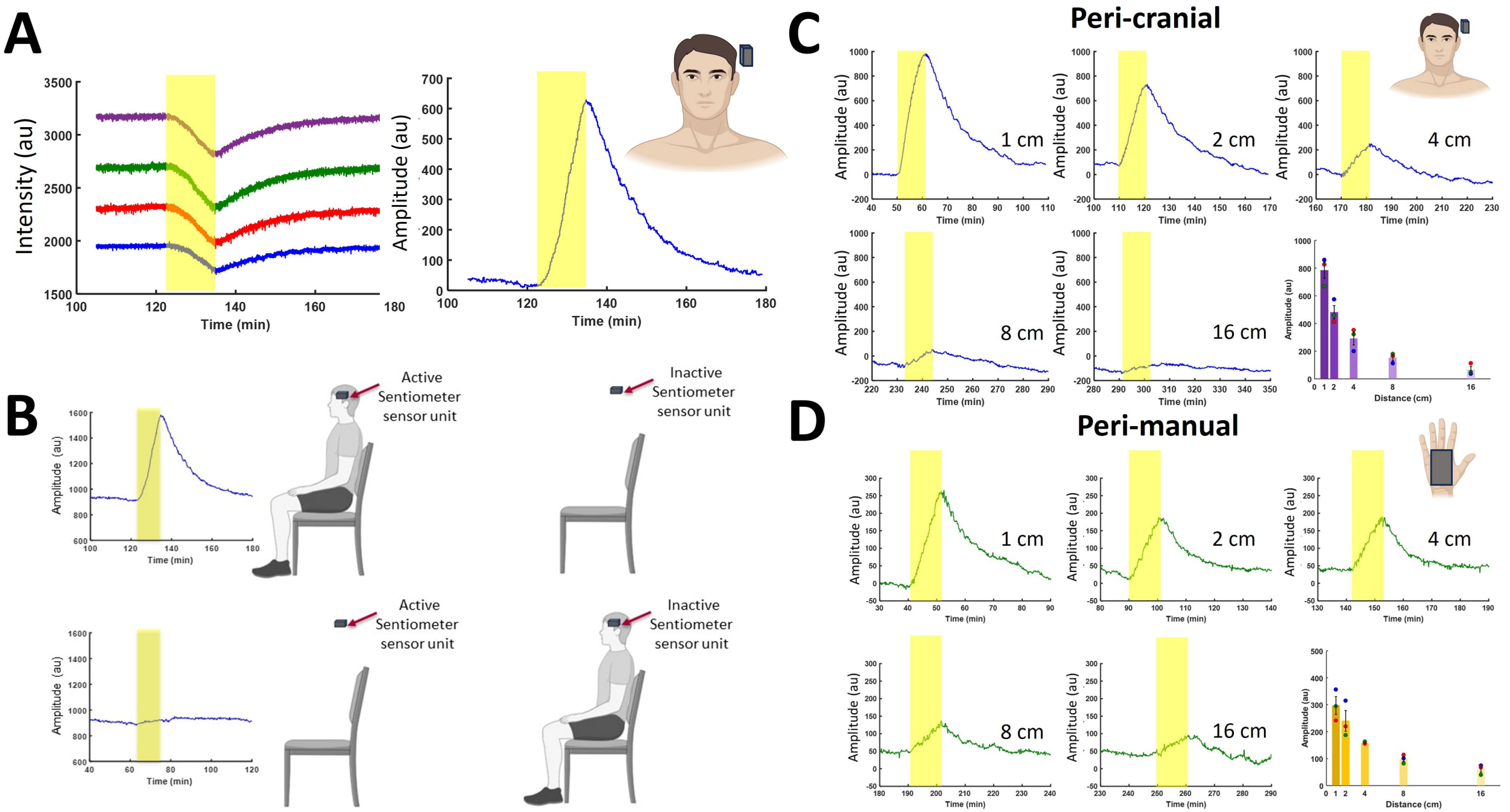
A
Intensity (au)
Time (min)
Amplitude (au)
Time (min)
B
Active Sentiometer sensor unit
Inactive Sentiometer sensor unit
Amplitude (au)
Time (min)
Active Sentiometer sensor unit
Inactive Sentiometer sensor unit
Amplitude (au)
Time (min)
C
Peri-cranial
1 cm
2 cm
4 cm
8 cm
16 cm
Amplitude (au)
Time (min)
Distance (cm)
D
Peri-manual
1 cm
2 cm
4 cm
8 cm
16 cm
Amplitude (au)
Time (min)
Distance (cm)

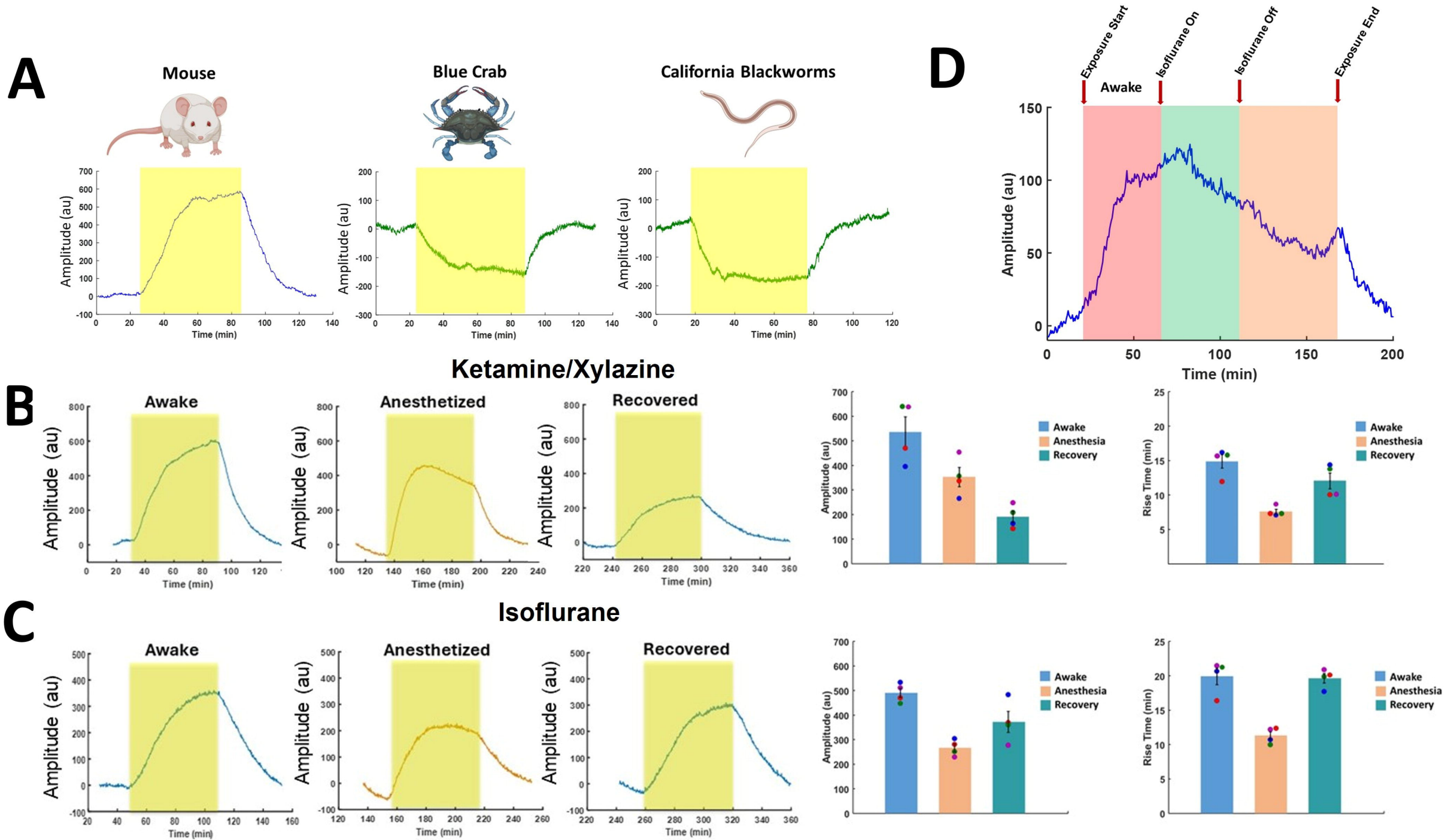
A
Mouse
Blue Crab
California Blackworms
Amplitude (au)
Time (min)
D
Exposure Start
Isoflurane On
Isoflurane Off
Exposure End
Awake
Amplitude (au)
Time (min)
Ketamine/Xylazine
B
Awake
Anesthetized
Recovered
Amplitude (au)
Time (min)
Awake
Anesthesia
Recovery
Amplitude (au)
Rise Time (min)
Isoflurane
C
Awake
Anesthetized
Recovered
Amplitude (au)
Time (min)
Awake
Anesthesia
Recovery
Amplitude (au)
Rise Time (min)

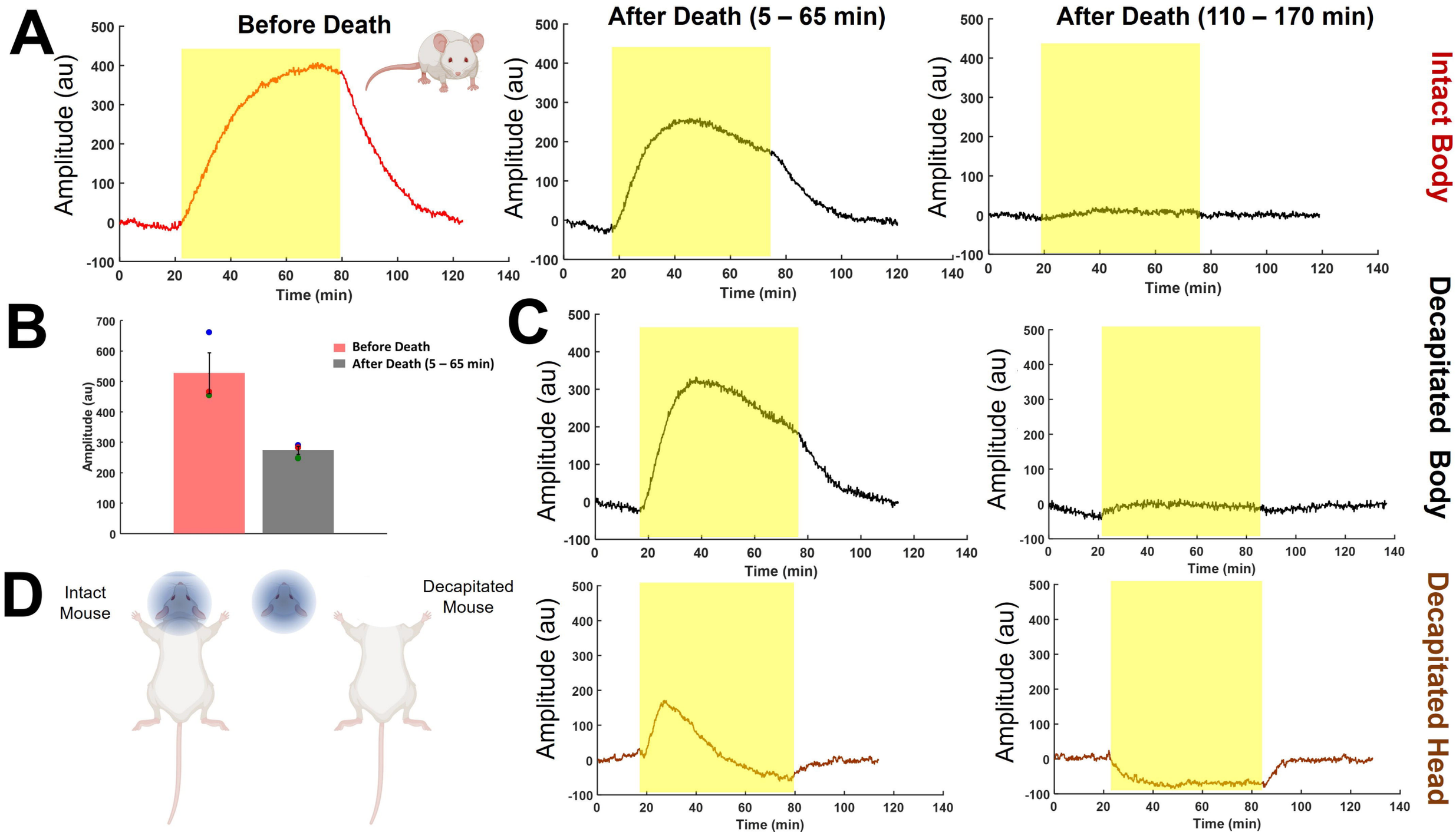
A
Before Death
After Death (5 – 65 min)
After Death (110 – 170 min)
Intact Body
Decapitated Body
Decapitated Head
Amplitude (au)
Time (min)
B
Before Death
After Death (5 – 65 min)
Amplitude (au)
C
D
Intact Mouse
Decapitated Mouse

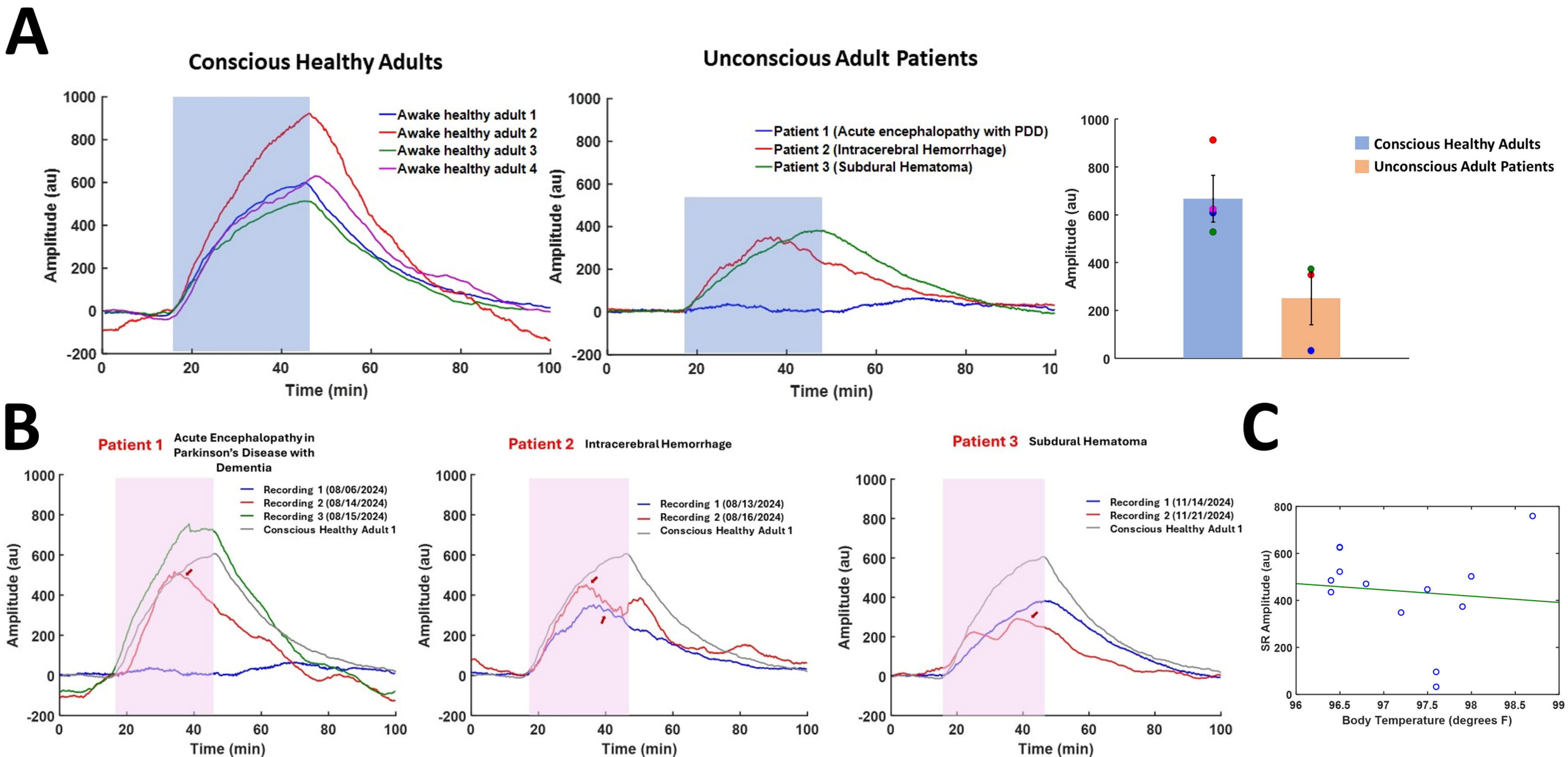
A
Conscious Healthy Adults
Awake healthy adult 1
Awake healthy adult 2
Awake healthy adult 3
Awake healthy adult 4
Amplitude (au)
Time (min)
Unconscious Adult Patients
Patient 1 (Acute encephalopathy with PDD)
Patient 2 (Intracerebral Hemorrhage)
Patient 3 (Subdural Hematoma)
Conscious Healthy Adults
Unconscious Adult Patients
B
Patient 1 Acute Encephalopathy in Parkinson's Disease with Dementia
Recording 1 (08/06/2024)
Recording 2 (08/14/2024)
Recording 3 (08/15/2024)
Conscious Healthy Adult 1
Patient 2 Intracerebral Hemorrhage
Recording 1 (08/13/2024)
Recording 2 (08/16/2024)
Conscious Healthy Adult 1
Patient 3 Subdural Hematoma
Recording 1 (11/14/2024)
Recording 2 (11/21/2024)
Conscious Healthy Adult 1
C
SR Amplitude (au)
Body Temperature (degrees F)